

Mutually Synchronized Macroscopic Josephson Oscillations Demonstrated by Polarization Analysis of Superconducting Terahertz Emitters

M. Tsujimoto^{1,2,*}, S. Fujita,³ G. Kuwano,² K. Maeda,³ A. Elarabi^{3,†}, J. Hawecker,⁴ J. Tignon^{3,‡}, J. Mangeney,⁴ S.S. Dhillon,⁴ and I. Kakeya^{3,†}

¹*Faculty of Pure and Applied Sciences, University of Tsukuba, 1-1-1 Tennodai, Tsukuba, Ibaraki 305-8573, Japan*

²*Graduate School of Pure and Applied Sciences, University of Tsukuba, 1-1-1 Tennodai, Tsukuba, Ibaraki 305-8573, Japan*

³*Department of Electronic Science and Engineering, Kyoto University, Nishikyo-ku, Kyoto 615-8510, Japan*

⁴*Laboratoire de Physique de l'Ecole normale supérieure, ENS, Université PSL, CNRS, Sorbonne Université, Université de Paris, F-75005 Paris, France*



(Received 9 March 2020; accepted 9 April 2020; published 13 May 2020)

We demonstrate mutual synchronization of Josephson oscillations in multiple stacks of intrinsic Josephson junctions of the cuprate superconductor $\text{Bi}_2\text{Sr}_2\text{CaCu}_2\text{O}_{8+\delta}$. Detailed analysis of the full polarization parameters allows the determination of a phase correlation between the stacks: a simultaneous emission state is described by a linear combination of individual emission states with a phase retardation. This proves that the stacks are coupled via a Josephson plasma in a superconducting substrate and that the coupling matrices can be extracted from polarization analyses. Our findings suggest a route towards the realization of high-power terahertz sources based on the synchronization of a large number of intrinsic Josephson junctions.

DOI: 10.1103/PhysRevApplied.13.051001

The observation of electromagnetic (EM) radiation in the terahertz frequency range emitted from a stack (mesa) of intrinsic Josephson junctions (IJJs) [1] in $\text{Bi}_2\text{Sr}_2\text{CaCu}_2\text{O}_{8+\delta}$ (Bi-2212) highlights the potential of such materials in monolithically fabricated solid-state terahertz sources [2–5]. The mutual synchronization of IJJ mesas has been demonstrated to produce output powers of up to 0.6 mW [6], where the maximum output power exceeds the sum of the individual emission powers. Although a numerical study suggests a possible coupling between the mesas through the Bi-2212 substrate [7], there is no direct experimental evidence showing the mutual synchronization. So far, to investigate these phenomena with multidegree of freedom, the frequency and intensity of the emitted EM wave have been considered good measures. Besides these characteristics, the polarization includes rich information for characterizing the Josephson plasma wave (JPW) polarized along the *c* axis inside a mesa [8,9]. Since a JPW is converted to a polarized photon according to the mesa geometry [10–13], perfect polarization is the hallmark of coherent excitation of the JPW.

*tsujimoto@ims.tsukuba.ac.jp

†kakeya@kuee.kyoto-u.ac.jp

‡Present address: Okinawa Institute of Science and Technology Graduate University, Onna, Okinawa 904-0495, Japan.

In this work we demonstrate synchronization of macroscopic Josephson oscillations in two simultaneously biased mesas coupled via a superconducting base crystal by measuring complete Stokes polarization parameters. Our focus is on the polarization of photons emitted from individual mesas and arrays of mesas. Most importantly, we observe a drastic change in the axial ratio for the simultaneous emission. This suggests the possibility of active control of the synchronization in mesa arrays, which is the most promising way to increase the integrated output power.

Mesas $100 \times 400 \mu\text{m}^2$ in size with two silver strip electrodes were milled from a Bi-2212 crystal by photolithography and argon milling methods. In Fig. 1(a) we show an optical microscopy image of the Bi-2212 mesa array. We refer to the two mesas as A1 and A2. Profile measurements using atomic force microscopy (Keyence Corporation, model VN-8000) demonstrate that the mesas vary marginally in size. The widths of A1 and A2 are measured as $94 \mu\text{m}$ and $91 \mu\text{m}$, respectively, with thicknesses of $1.4 \mu\text{m}$, corresponding to 910 IJJs.

The current-voltage characteristics (IVCs) for A1 and A2 show the large hysteresis typical of underdamped Josephson junctions [14]. Simultaneous emission occurs when A1 and A2 are biased in parallel. Hereinafter, we refer to the parallel connection as $A1 \parallel A2$. The maximum intensity is obtained at 16.8 mA, which is higher than the sum of the bias currents for the maximum emission powers

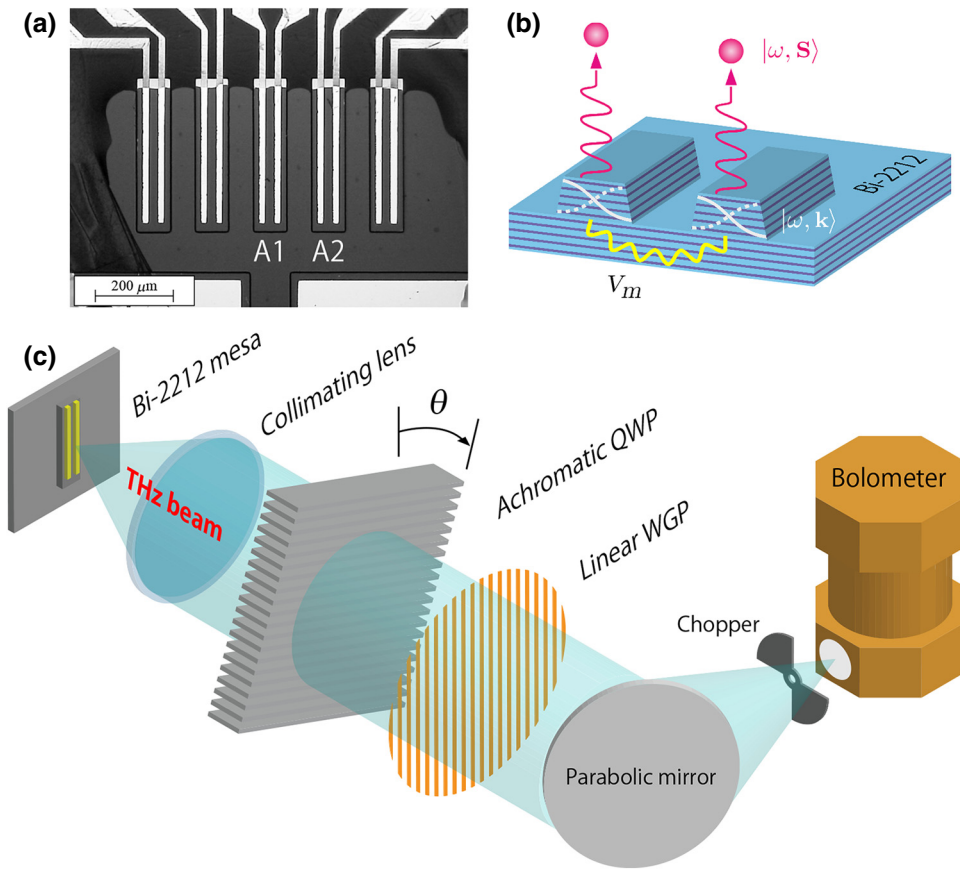


FIG. 1. (a) Optical microscopy image of the Bi-2212 mesa array. (b) Schematic view of the synchronized array. (c) Schematic of the optical configuration for Stokes parameter measurement.

of A1 and A2 individually. Also, the maximum intensity for $A_1 \parallel A_2$ is almost half of that for A2. This can be explained by considering the local temperature increase [15–21]. Benseman *et al.* [6] demonstrated that the self-heating effect limits the power output and in fact may prevent synchronization among multiple mesas. A variety of studies on the cavity resonance effect have demonstrated that spontaneous synchronization among stacked IJJs is accompanied by the formation of standing EM waves inside the Bi-2212 mesa [2,22–26]. For a thin rectangular mesa of width w and length ℓ , the cavity frequency for a transverse magnetic (mp) mode is given by $f_{mp}^r = (c_0/2n)\sqrt{(m/w)^2 + (p/\ell)^2}$, where the two indices m and p correspond to the numbers of electric field nodes in the width and length directions, respectively, and $n = 4.2$ is the experimentally obtained refractive index [24,27]. Here, the radiation frequencies measured using Fourier transform interferometry ranged continuously from 0.56 to 0.66 THz depending on the bias point [14]. These values are in good agreement with the calculated f_{1p}^r for $0 < p < 6$. If we assume that $m \geq 2$, the calculated f_{mp}^r values fail to coincide with the observed values for any p . Hence, only one EM node is present along the mesa width, and a nonzero p value is expected to produce an elliptical polarization.

Here, we present the measurements of the Stokes parameters, which allow for the quantitative analysis of polarized photons emitted from individual mesas and from synchronized arrays [14]. In Fig. 1(b) we show a schematic view of the synchronized array. Measurement was performed by allowing the polarized radiation to propagate sequentially through two polarizing elements: a quarter-wave plate (QWP) and a linear wire-grid polarizer (WGP). The QWP consists of a stack of parallel metal-plate waveguides [28]. We use terahertz time-domain spectroscopy [29,30] to verify that the QWP works correctly in the emission frequency range around 0.6 THz [14]. In Fig. 1(c) we show the measurement configuration. The QWP can be rotated through an angle θ and is followed by a fixed WGP whose transmission axis is fixed in the width direction ($\theta = 0^\circ$).

In Figs. 2(a) and 2(b) we show polar plots of the bolometer output for A1 and A1 \parallel A2, respectively, as a function of θ at the bias conditions that result in the maximum output powers. The error bars in the radial direction correspond to fluctuations in the bolometer output signal, mostly owing to background noise. The four independent Stokes parameters, S_0 , S_1 , S_2 , and S_3 , which are summarized in Table SI of the Supplemental Material [14], are obtained from this data. The solid lines shown in Figs. 2(a) and 2(b) represent the calculated results using the four Stokes

parameters. The experimental data are slightly asymmetric with respect to both the major and minor axes. This is due to the imperfect alignment of the parallel metal-plate waveguides in the QWP. Nevertheless, the calculation results fit the experimental data within the error bars.

The E -field vector at the detection plane is given by $\mathbf{E}(t) = E_{0x}e^{i(\omega t+\delta_x)}\mathbf{i} + E_{0y}e^{i(\omega t+\delta_y)}\mathbf{j}$, where the x and y axes are parallel to the mesa width and length, respectively, t represents time, E_{0x} and E_{0y} are the respective amplitudes, and δ_x and δ_y are the respective phase constants. Figures 2(c) and 2(d) show the corresponding polarization ellipses for A1 (red), A2 (blue), and A1 \parallel A2 (green). The fourth Stokes parameter S_3 determines the helicity of the photons: a positive (negative) S_3 indicates left (right)-handed helicity with respect to the direction of propagation. Note that the E field rotates clockwise (counterclockwise) for left (right)-handed helicity from the viewpoint of

the detector. The arrows on the ellipses indicate the direction of the E -field rotation. For both mesas, the major axis of the polarization ellipse is oriented along the x axis, i.e., $-\pi/4 < \psi < \pi/4$, which is consistent with excitation of (1p) cavity modes.

In the pioneering study of EM wave emission from an IJJ mesa, it is demonstrated that the emission from rectangular mesas is linearly polarized along the mesa width [2]. The present results suggest, however, that the emitted waves are elliptically polarized with a finite axial ratio at an arbitrary orientation angle. We stress that these polarization parameters contain information essential for understanding the electromagnetism inside the emitting mesa. For example, the orientation angle ψ is derived from the phase difference $\delta_{xy} = \delta_x - \delta_y$, namely, $\delta_{xy} = \pm\pi/2$ gives $\psi = 0$ and $\delta_{yx} = 0$ gives $\psi = 30^\circ$ for $E_{0x}^2/E_{0y}^2 \sim 3$. We also find that the actual polarization parameters are, in

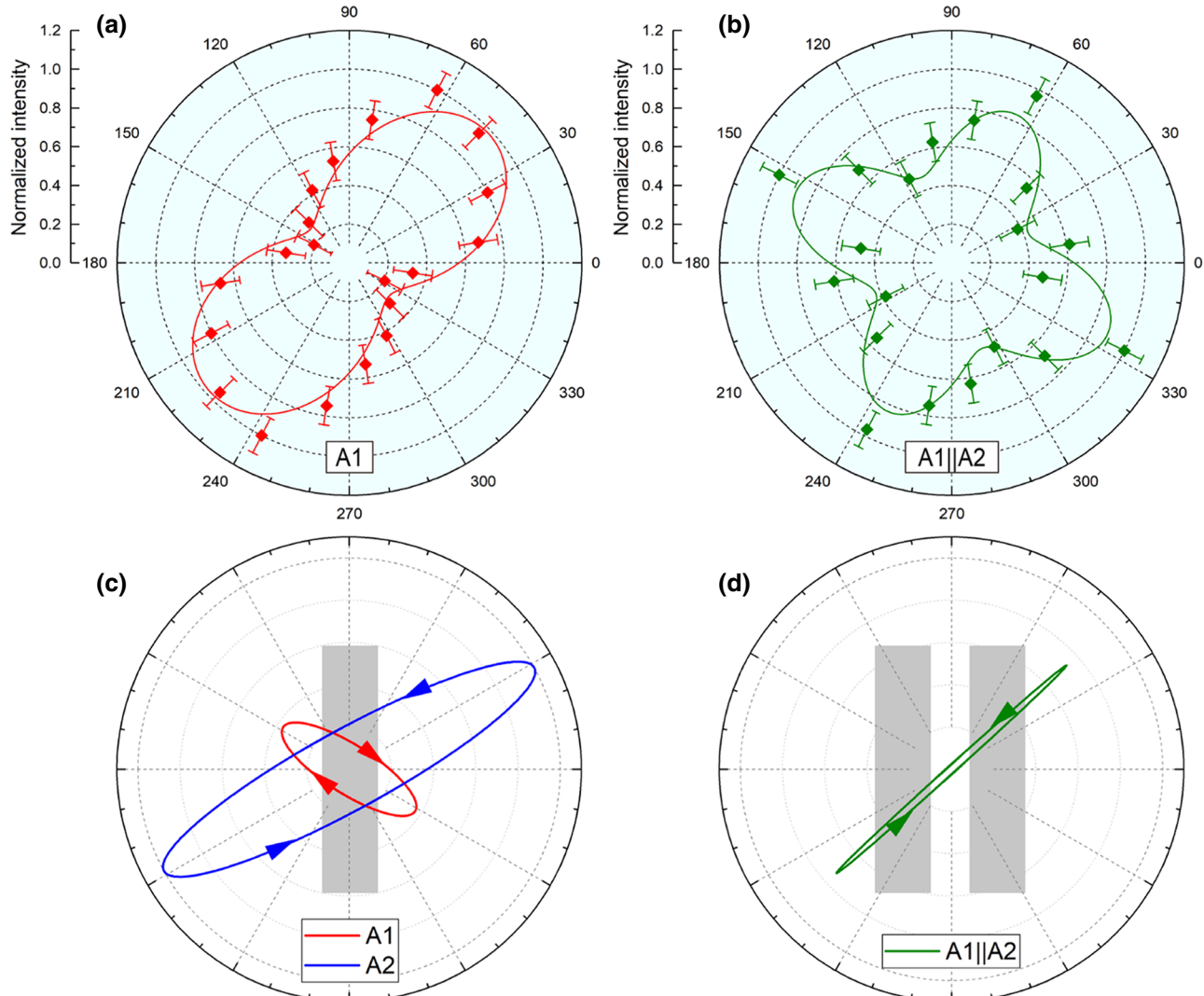


FIG. 2. Polar plots of the maximum bolometer output as a function of the QWP angle θ for (a) A1 and (b) A1 \parallel A2. The solid lines represent results calculated using the Stokes parameters. Polarization ellipses for (c) A1 (red) and A2 (blue), and (d) A1 \parallel A2.

fact, dependent on the bias condition and the bath temperature T_b . Nevertheless, the observed E_{0x} was greater than E_{0y} in all cases, directly suggesting the predominance of the (1p) cavity mode for elongated rectangular mesas.

When two mesas are biased to emit simultaneously, the far-field waves should be described in terms of the superposition of the E fields generated from each mesa. Thus, the total E field depends on the phase difference between the macroscopic Josephson oscillations. The observed pattern for $A1 \parallel A2$ shown in Fig. 2(b) exhibits four-fold symmetry with respect to θ , suggesting that the two mesas generate photons synchronously. It is likely that ψ and the helicity for $A1 \parallel A2$ are dominated by the photon from $A2$, which emits more intensively than $A1$ [see Fig. 2(c)]. Most importantly, we find that the axial ratio increases significantly from 2 for the individual emissions to 24 for the simultaneous emission. We propose that this pronounced effect on the axial ratio is an indication of the phase synchronization between the two mesas as a result of EM coupling.

We observe the same behavior from other mesas shown in Fig. 1(a) and another supplemental sample, where each mesa shows slightly different polarization depending on the geometrical configuration [14]. The amplitude ratio E_{0x}/E_{0y} explains the predominance of cavity resonances in the width direction over those in the length direction. Since we inject the dc bias current into $A1$ and $A2$ using a left-strip electrode, as shown in Fig. 1(a), the resonance in the width direction may be degraded by a nonuniform current distribution in the mesa [20,31]. This explanation is supported by the observation that $E_{0x}/E_{0y} = 1.4$ for $A1$ and, in contrast, 2.0 for supplemental mesas with a symmetrical electrode configuration [14]. This technique allows for dynamic control of polarization by adjusting the current distribution in the mesa.

In Fig. 3(a) we plot the polarization ellipses obtained by calculating the locus of $\mathbf{E}(t)$. According to antenna theory for a transverse magnetic cavity, E_{0x} (or E_{0y}) is

proportional to the magnitude of the magnetic currents parallel to the y axis (or x axis). Hence, in order to calculate $\mathbf{E}(t)$, we assume that the anisotropy is equal to the inverse mesa aspect, i.e., $E_{0x}/E_{0y} = \ell/w$. This geometrical effect coincides with the numerical simulation for a locally heated square IJJ mesa [32]. By comparing Fig. 3(a) with Fig. 2(c), we can estimate δ_{yx} to be $3\pi/4$ (135°) for $A1$ and $-\pi/4$ (-45°) for $A2$.

Let us describe our results in terms of quantum mechanics. The quantum-mechanically-superposed state of the photon emitted from the parallel-biased mesa array of $A1 \parallel A2$ can be described as

$$|\omega_{A1 \parallel A2}, S_{A1 \parallel A2}\rangle = \alpha |\omega_{A1}, S_{A1}\rangle + \beta |\omega_{A2}, S_{A2}\rangle,$$

where S_i ($i = A1, A2$, or $A1 \parallel A2$) represents the Stokes vector as a quantum number. Two complex numbers α and β represent the probability amplitudes (i.e., $|\alpha|^2 + |\beta|^2 = 1$) and phases of the unperturbed states $|\omega_{A1}, S_{A1}\rangle$ and $|\omega_{A2}, S_{A2}\rangle$, respectively. According to the dispersion relation of the transverse JPW [33,34], angular frequencies ω_{A1} and ω_{A2} are determined by the wave numbers \mathbf{k}_{A1} and \mathbf{k}_{A2} of the Josephson plasmons (quantized JPW) [12,35] independently of the polarization. Our concern is finding the 4×4 perturbation matrix V_m that satisfies

$$\begin{pmatrix} |\omega'_{A1}, \mathbf{k}'_{A1}\rangle \\ |\omega'_{A2}, \mathbf{k}'_{A2}\rangle \end{pmatrix} = V_m \begin{pmatrix} |\omega_{A1}, \mathbf{k}_{A1}\rangle \\ |\omega_{A2}, \mathbf{k}_{A2}\rangle \end{pmatrix}.$$

Here, intermesa coupling V_m causes perturbation and may include nondiagonal elements, which involve a general question in nonlinear physics regarding the symmetry of the matrix.

In Fig. 3(b) we show polarization $S_{A1 \parallel A2}$ calculated by taking the superposition into consideration. We use the actual intensity ratio obtained by measurement. The orientation angle in the range $0 < \psi < \pi/2$ is in good agreement with Fig. 2(d). It is noteworthy that the modulus $|\beta/\alpha|$ represents the degree of interaction between

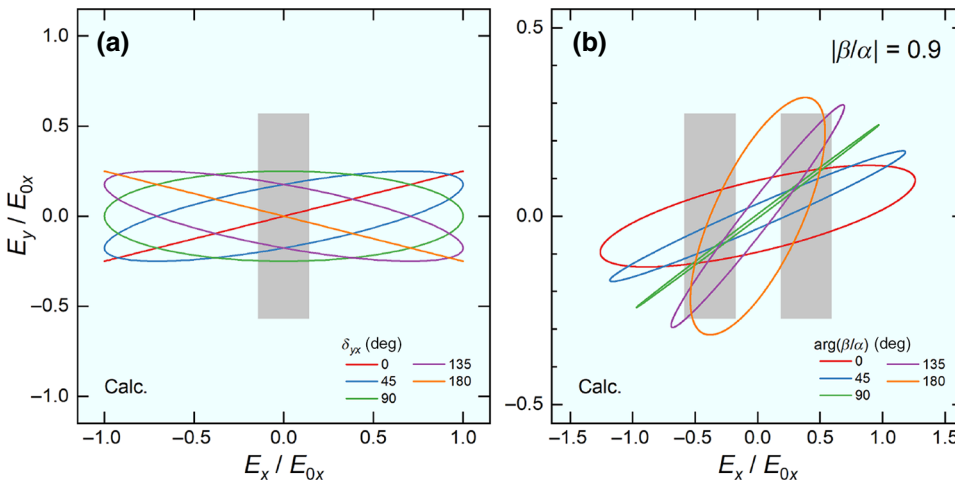


FIG. 3. Calculation of the polarization ellipse for (a) a single mesa and (b) two arrayed mesas.

the two mesas and $|\beta/\alpha| = 0.9$ coincides with our results. Meanwhile, the argument of β/α corresponds to the phase difference between A1 and A2.

In Fig. 4 we show the variation of axial ratio as a function of $\arg(\beta/\alpha)$. As indicated by arrows, two singular states exhibiting perfect polarization are emitted when $|\beta/\alpha| < 0.9$. For example, two singular states with very large axial ratio can be observed at $\arg(\beta/\alpha) = 45^\circ$ and at 135° when $|\beta/\alpha| = 0.7$. We suggest that such perfect polarization is attributed to coherent excitation of the Josephson plasmon. See the Supplemental Material [14] for $|\beta/\alpha|$ -dependence of $S_{A1||A2}$.

The origin of intermesa coupling V_m arises from the propagation of JPWs through the Bi-2212 base crystal, as depicted in Fig. 1(b). The inset of Fig. 4 shows a schematic cross-sectional view of the mesa array. The dashed line in Fig. 4 represents the phase delay $2\pi D/\lambda'$ due to the finite propagation time, where $D = 58 \mu\text{m}$ is the interspace between the two mesas and $\lambda' = \lambda/n$ is the effective wavelength. We assume that JPWs can propagate from one mesa to another mesa through the base crystal and diffract at the mesa edge. This situation strongly supports the view that the base crystal can mediate the EM interaction [6,7], the mechanism of which has been unclear in previous works. Furthermore, we find that the total intensity of simultaneous emission S_0 reaches a maximal value as $2\pi D/\lambda'$ coincides with a multiple of $\arg(\beta/\alpha)$ [14].

In conclusion, we demonstrate the synchronization of macroscopic Josephson oscillations in two simultaneously biased Bi-2212 IJJ mesas coupled via a base crystal by measuring the complete Stokes parameters. We use an achromatic QWP and a linear WGP to analyze the orthogonal components of the emitted E fields. We prove that the coherent radiation is elliptically polarized with the major axis oriented in the width direction. Most importantly, we observe a significant increase in the axial ratio for simultaneous emission, suggesting that Josephson plasma in the

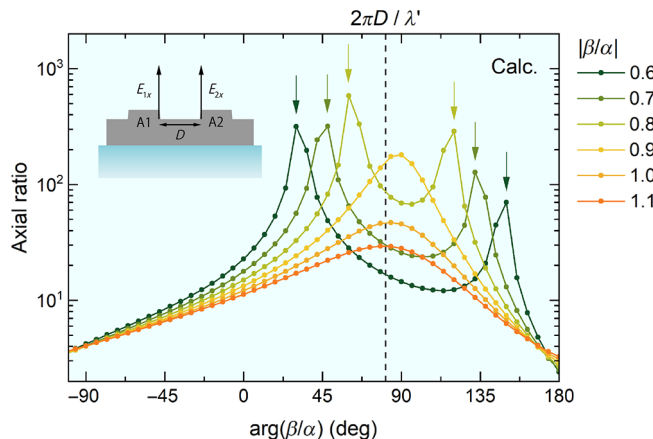


FIG. 4. Calculation of the axial ratio as a function of $\arg(\beta/\alpha)$. Inset: schematic side view of the Bi-2212 mesa array.

Bi-2212 base crystal can mediate an interaction between two individual mesas. This finding represents a possible means of manipulating the synchronization of IJJ arrays, and is the most promising way to increase the integrated radiation power.

ACKNOWLEDGMENTS

This work was supported by the Japan Society for the Promotion of Science (JSPS) KAKENHI (Grants No. 19H02540 and No. 15KK0204), JSPS-Centre national de la recherche scientifique (CNRS) Bilateral Program (Grant No. 120192908), and the Program to Disseminate the Tenure Tracking System at the University of Tsukuba. The Bi-2212 single crystal was provided by Y. Nakagawa at Kyoto University. The authors thank H. Asai, S. Kawabata, M. Machida, and T. Koyama for their valuable discussions.

- [1] R. Kleiner, F. Steinmeyer, G. Kunkel, and P. Müller, Intrinsic Josephson Effects in $\text{Bi}_2\text{Sr}_2\text{CaCu}_2\text{O}_8$ Single Crystals, *Phys. Rev. Lett.* **68**, 2394 (1992).
- [2] L. Ozyuzer, A. E. Koshelev, C. Kurter, N. Gopalsami, Q. Li, M. Tachiki, K. Kadokawa, T. Yamamoto, H. Minami, H. Yamaguchi, T. Tachiki, K. E. Gray, W.-K. Kwok, and U. Welp, Emission of coherent THz radiation from superconductors, *Science* **318**, 1291 (2007).
- [3] U. Welp, K. Kadokawa, and R. Kleiner, Superconducting emitters of THz radiation, *Nat. Photonics* **7**, 702 (2013).
- [4] I. Kakeya and H. Wang, Terahertz-wave emission from Bi2212 intrinsic Josephson junctions: A review on recent progress, *Supercond. Sci. Technol.* **29**, 073001 (2016).
- [5] T. Kashiwagi, H. Kubo, K. Sakamoto, T. Yuasa, Y. Tanabe, C. Watanabe, T. Tanaka, Y. Komori, R. Ota, G. Kuwano, K. Nakamura, T. Katsuragawa, M. Tsujimoto, T. Yamamoto, R. Yoshizaki, H. Minami, K. Kadokawa, and R. A. Klemm, The present status of high- T_c superconducting terahertz emitters, *Supercond. Sci. Technol.* **30**, 074008 (2017).
- [6] T. M. Benseman, K. E. Gray, A. E. Koshelev, W.-K. Kwok, U. Welp, H. Minami, K. Kadokawa, and T. Yamamoto, Powerful terahertz emission from $\text{Bi}_2\text{Sr}_2\text{CaCu}_{2+\delta}$ mesa arrays, *Appl. Phys. Lett.* **103**, 022602 (2013).
- [7] S. Z. Lin and A. E. Koshelev, Synchronization of Josephson oscillations in a mesa array of $\text{Bi}_2\text{Sr}_2\text{CaCu}_{2+\delta}$ through the Josephson plasma waves in the base crystal, *Phys. C: Supercond. Appl.* **491**, 24 (2013).
- [8] A. Elarabi, Y. Yoshioka, M. Tsujimoto, and I. Kakeya, Monolithic Superconducting Emitter of Tunable Circularly Polarized Terahertz Radiation, *Phys. Rev. Appl.* **8**, 064034 (2017).
- [9] A. Elarabi, Y. Yoshioka, M. Tsujimoto, and I. Kakeya, Circularly polarized terahertz radiation monolithically generated by cylindrical mesas of intrinsic Josephson junctions, *Appl. Phys. Lett.* **113**, 052601 (2018).
- [10] T. Koyama, H. Matsumoto, M. Machida, and K. Kadokawa, In-phase electrodynamics and terahertz wave emission in extended intrinsic Josephson junctions, *Phys. Rev. B* **79**, 104522 (2009).

- [11] X. Hu and S. Lin, Cavity phenomena in mesas of cuprate high- T_c superconductors under voltage bias, *Phys. Rev. B* **80**, 064516 (2009).
- [12] S. Savel'ev, V. A. Yampol'skii, A. L. Rakhmanov, and F. Nori, Terahertz Josephson plasma waves in layered superconductors: Spectrum, generation, nonlinear and quantum phenomena, *Rep. Prog. Phys.* **73**, 026501 (2010).
- [13] R. A. Klemm and K. Kadowaki, Output from a Josephson stimulated terahertz amplified radiation emitter, *J. Phys.: Condens. Matter* **22**, 375701 (2010).
- [14] See Supplemental Material at <http://link.aps.org/supplemental/10.1103/PhysRevApplied.13.051001> for details of methods and additional data to support main text.
- [15] H. Wang, S. Guénon, J. Yuan, A. Iishi, S. Arisawa, T. Hatano, T. Yamashita, D. Koelle, and R. Kleiner, Hot Spots and Waves in $\text{Bi}_2\text{Sr}_2\text{CaCu}_2\text{O}_8$ Intrinsic Josephson Junction Stacks: A Study by Low Temperature Scanning Laser Microscopy, *Phys. Rev. Lett.* **102**, 017006 (2009).
- [16] H. B. Wang, S. Guénon, B. Gross, J. Yuan, Z. G. Jiang, Y. Y. Zhong, M. Grünzweig, A. Iishi, P. H. Wu, T. Hatano, D. Koelle, and R. Kleiner, Coherent Terahertz Emission of Intrinsic Josephson Junction Stacks in the Hot Spot Regime, *Phys. Rev. Lett.* **105**, 057002 (2010).
- [17] B. Gross, S. Guénon, J. Yuan, M. Y. Li, J. Li, A. Ishii, R. G. Mints, T. Hatano, P. H. Wu, D. Koelle, H. B. Wang, and R. Kleiner, Hot-spot formation in stacks of intrinsic Josephson junctions in $\text{Bi}_2\text{Sr}_2\text{CaCu}_2\text{O}_8$, *Phys. Rev. B* **86**, 094524 (2012).
- [18] T. M. Benseman, A. E. Koshelev, W.-K. Kwok, U. Welp, V. K. Vlasko-Vlasov, K. Kadowaki, H. Minami, and C. Watanabe, Direct imaging of hot spots in $\text{Bi}_2\text{Sr}_2\text{CaCu}_2\text{O}_{8+\delta}$ mesa terahertz sources, *J. Appl. Phys.* **113**, 133902 (2013).
- [19] H. Minami, C. Watanabe, K. Sato, S. Sekimoto, T. Yamamoto, T. Kashiwagi, R. A. Klemm, and K. Kadowaki, Local SiC photoluminescence evidence of hot spot formation and sub-THz coherent emission from a rectangular $\text{Bi}_2\text{Sr}_2\text{CaCu}_2\text{O}_{8+\delta}$ mesa, *Phys. Rev. B* **89**, 054503 (2014).
- [20] M. Tsujimoto, H. Kambara, Y. Maeda, Y. Yoshioka, Y. Nakagawa, and I. Kakeya, Dynamic Control of Temperature Distributions in Stacks of Intrinsic Josephson Junctions in $\text{Bi}_2\text{Sr}_2\text{CaCu}_2\text{O}_{8+\delta}$ for Intense Terahertz Radiation, *Phys. Rev. Appl.* **2**, 044016 (2014).
- [21] T. M. Benseman, A. E. Koshelev, V. Vlasko-Vlasov, Y. Hao, W.-K. Kwok, U. Welp, C. Keiser, B. Gross, M. Lange, D. Kölle, R. Kleiner, H. Minami, C. Watanabe, and K. Kadowaki, Current Filamentation in Large $\text{Bi}_2\text{Sr}_2\text{CaCu}_2\text{O}_{8+\delta}$ Mesa Devices Observed via Luminescent and Scanning Laser Thermal Microscopy, *Phys. Rev. Appl.* **3**, 044017 (2015).
- [22] M. Tsujimoto, K. Yamaki, K. Deguchi, T. Yamamoto, T. Kashiwagi, H. Minami, M. Tachiki, K. Kadowaki, and R. A. Klemm, Geometrical Resonance Conditions for THz Radiation from the Intrinsic Josephson Junctions in $\text{Bi}_2\text{Sr}_2\text{CaCu}_2\text{O}_{8+\delta}$, *Phys. Rev. Lett.* **105**, 037005 (2010).
- [23] T. Kashiwagi, K. Yamaki, M. Tsujimoto, K. Deguchi, N. Orita, T. Koike, R. Nakayama, H. Minami, T. Yamamoto, R. A. Klemm, M. Tachiki, and K. Kadowaki, Geometrical full-wavelength resonance mode generating terahertz waves From a single-crystalline $\text{Bi}_2\text{Sr}_2\text{CaCu}_2\text{O}_{8+\delta}$ rectangular mesa, *J. Phys. Soc. Jpn.* **80**, 094709 (2011).
- [24] M. Tsujimoto, I. Kakeya, T. Kashiwagi, H. Minami, and K. Kadowaki, Cavity mode identification for coherent terahertz emission from high- T_c superconductors, *Opt. Express* **24**, 4591 (2016).
- [25] T. Kashiwagi, T. Yuasa, Y. Tanabe, T. Imai, G. Kuwano, R. Ota, K. Nakamura, Y. Ono, Y. Kaneko, M. Tsujimoto, H. Minami, T. Yamamoto, R. A. Klemm, and K. Kadowaki, Improved excitation mode selectivity of high- T_c superconducting terahertz emitters, *J. Appl. Phys.* **124**, 033901 (2018).
- [26] H. Zhang *et al.*, Resonant Cavity Modes in $\text{Bi}_2\text{Sr}_2\text{CaCu}_2\text{O}_{8+x}$ Intrinsic Josephson Junction Stacks, *Phys. Rev. Appl.* **11**, 044004 (2019).
- [27] K. Kadowaki, M. Tsujimoto, K. Yamaki, T. Yamamoto, T. Kashiwagi, H. Minami, M. Tachiki, and R. A. Klemm, Evidence for a dual-source mechanism of terahertz radiation from rectangular mesas of single crystalline $\text{Bi}_2\text{Sr}_2\text{CaCu}_2\text{O}_{8+\delta}$ intrinsic Josephson junctions, *J. Phys. Soc. Jpn.* **79**, 023703 (2010).
- [28] M. Nagai, N. Mukai, Y. Minowa, M. Ashida, T. Suzuki, J. Takayanagi, and H. Ohtake, Achromatic wave plate in THz frequency region based on parallel metal plate waveguides with a pillar array, *Opt. Express* **23**, 4641 (2015).
- [29] J. Madeo, N. Jukam, D. Oustinov, M. Rosticher, R. Rung-sawang, J. Tignon, and S. Dhillon, Frequency tunable terahertz interdigitated photoconductive antennas, *Electron. Lett.* **46**, 611 (2010).
- [30] K. Maussang, A. Brewer, J. Palomo, J.-M. Manceau, R. Colombelli, I. Sagnes, J. Mangeney, J. Tignon, and S. S. Dhillon, Echo-less photoconductive antenna sources for high-resolution terahertz time-domain spectroscopy, *IEEE Trans. Terahertz Sci. Technol.* **6**, 20 (2016).
- [31] I. Kakeya, Y. Omukai, T. Yamamoto, K. Kadowaki, and M. Suzuki, Effect of thermal inhomogeneity for terahertz radiation from intrinsic Josephson junction stacks of $\text{Bi}_2\text{Sr}_2\text{CaCu}_2\text{O}_{8+\delta}$, *Appl. Phys. Lett.* **100**, 242603 (2012).
- [32] H. Asai and S. Kawabata, Control of circularly polarized THz wave from intrinsic Josephson junctions by local heating, *Appl. Phys. Lett.* **110**, 132601 (2017).
- [33] M. Tachiki, T. Koyama, and S. Takahashi, Electromagnetic phenomena related to a low-frequency plasma in cuprate superconductors, *Phys. Rev. B* **50**, 7065 (1994).
- [34] K. Kadowaki, I. Kakeya, M. B. Gaifullin, T. Mochiku, S. Takahashi, T. Koyama, and M. Tachiki, Longitudinal Josephson-plasma excitation in $\text{Bi}_2\text{Sr}_2\text{CaCu}_2\text{O}_{8+\delta}$: Direct observation of the Nambu-Goldstone mode in a superconductor, *Phys. Rev. B* **56**, 5617 (1997).
- [35] T. Koyama, Quantum theory for the transverse Josephson plasma in high- T_c superconductors, *J. Phys. Soc. Jpn.* **68**, 3062 (1999).